Radial Resistance Estimation of Non-Insulated HTS Magnets

J.P.M Ellingham[1], R. Mataira[1], T. Simpson[1], S. Venuturumilli[1], and N. Zhou[1]

[1]OpenStar Technologies, Wellington, New Zealand

***Abstract*—This paper presents an iterative method based on non-linear least squares for estimating the radial resistance of inductively coupled Non-insulated (NI) HTS coils. Although these results are of specific interest for levitated dipole fusion magnets, the estimation approach can be applied to any magnet composed of multiple NI HTS coils. OpenStar Technologies Ltd has developed a 5.6 T, 1.44 kA HTS magnet for a Levitated Dipole Reactor, named Junior, which consists of 14 individual NI coils. The proposed method was used to estimate the radial resistances in each of Junior's 14 coils, from multiple sets of experimental data. The results showed good agreement between the estimated parameters and experimental data. The largest estimated radial resistance for one coil was 3.93 μΩ. The smaller outer coils had the lowest estimated radial resistance, spanning from 360-770 nΩ. Estimates were consistent across all considered datasets for all coils, with the exception of coils 1A and 2B.**

***Index Terms*—Non-insulated HTS coil, Radial resistance, Levitated Dipole Reactor**

I. Introduction

OPENSTAR Technologies Ltd is developing a levitated dipole (LD) reactor [1] for fusion energy production, based on dipole confined plasmas first proposed by Hasegawa [2] and previously explored in devices such as the Levitated Dipole Experiment (LDX) [3] and Ring Trap 1 (RT 1) [4]. OpenStar's approach uses a fully high temperature superconducting (HTS), quasi persistent core magnet powered by an onboard HTS rectifier. Junior, OpenStar's first LD prototype magnet, is a 5.6 T, 1.44 kA HTS dipole comprising 14 series connected, non insulated [5], solder impregnated coils [6] operating at 30 K. Non insulated HTS coils provide inherent quench protection [7] through turn to turn current sharing, but accurate estimation of joint and radial (turn to turn) resistances is required to verify that the magnet meets design specifications. Mutual coupling between coils and the embedding of joint resistances within coil voltage measurements make this parameter identification challenging. This work presents a method to estimate coupled NI coil radial resistances from experimental data to address these challenges.

II. Physical System Architecture

Figure 1 shows Junior's coil layout, magnetic field distribution, numbering scheme, and series connections. The coil pack is symmetric about the z-axis [1]. All coils are wound from a mix of HTS tape suppliers, leading to small variations in axial height between 12.0 mm and 12.1 mm, as summarized in Table 1. Each coil is designed with a uniform turn thickness of 600 μm, while the turn composition is adjusted by varying the number of parallel HTS tapes and co-wind layers. Coils located in regions of higher magnetic field have reduced critical current and therefore employ more parallel HTS tapes.

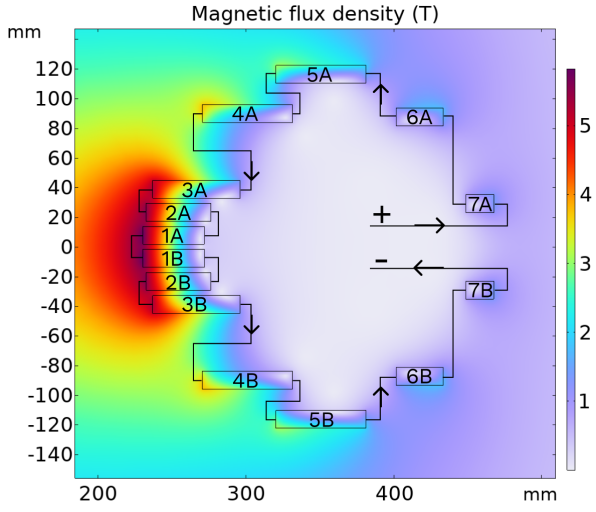

Fig. 1. Axi-symmetric cross-section of Junior showing magnetic field strength norm and coil arrangement. The positive terminal of the power supply connects to coil 7A and the negative terminal to coil 7B. [8]

TABLE I
Coil Geometry Specifications

Coils	a_1 (mm)	a_2 (mm)	b_1 (mm)	b_2 (mm)	# Turns
1A, 1B	230.2	270.7	2.0	14.0	68
2A, 2B	232.4	269.8	18.0	30.0	63
3A, 3B	236.9	295.9	34.0	46.0	99
4A, 4B	270.4	330.4	83.8	95.8	100
5A, 5B	320.1	380.1	110.2	122.2	100
6A, 6B	401.6	432.3	81.3	93.4	52
7A, 7B	448.5	466.4	23.1	35.2	30

As seen in Table 1, the Junior magnet consists of 14 solder impregnated non-insulated (NI) coils, as the magnet is primarily run as a DC quasi-persistent magnet. Being made of NI coils, series resistance and radial resistance, together with the inductance matrix, determine the overall electrical and dynamic behavior of the magnet. Series resistance is the sum of all resistive elements in the main current path between coils, including interface resistances at mechanical

[1]The number of turns in A/B coil pairs are unequal by 1-2 turns, resulting in an asymmetric mutual inductance matrix.

or indium joints and any additional solder joint resistances embedded within individual coils. Radial resistance represents the effective turn-to-turn resistance within non-insulated coils, providing current-sharing paths transverse to the series current.

Thus, the combination of finite radial resistance and negligible azimuthal resistance in the HTS tape allows NI coils to support both radial and azimuthal current paths. At the onset of a current transient, most of the transport current flows radially through turn-to-turn contacts, whereas in steady state it relaxes into an almost purely azimuthal path along the conductor. The effective radial resistance of an NI coil is set by its turn geometry and total turn count , which together determine the aggregate turn-to-turn contact resistance. A lumped-element equivalent circuit for a single-pancake NI coil, which can be extended to model multiple mutually coupled NI coils, is shown in Fig. 2 [9]. More sophisticated models combining finite-element and circuit approaches have also been proposed to capture NI behavior in greater detail [10] [11] [12]. However, for parameter identification in a multi-coil magnet, a simple lumped-circuit representation that includes mutual coupling between NI coils is preferred.

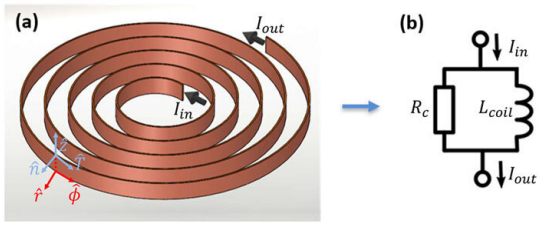

Fig. 2. (a) NI coil split into cylindrical coordinates. (b) The electrically equivalent lumped circuit model for an NI coil [9]

III. Equivalent Circuit Models

The lumped circuit model for a single NI coil can be used as a building block for the following equivalent circuit models (eqs. 2-7). Each of the 14 coils are inductively coupled, as described by the 14x14 mutual inductance matrix, $\mathbf{M}$. The inductance matrix was estimated using COMSOL Multiphysics [13] (Fig. 3). Equations can be derived using Kirchhoff's Voltage Law (KVL) and placed in Linear Time Invariant (LTI) state space form. Note, HTS resistance, described by the E-J power law (eq. 1) was neglected in the following circuit models. This assumption is valid if the ratio of transport current to critical current is low. The addition of this term makes the fitting process far more complicated, since it is highly non-linear with the n value and I_c are itself a function of the azimuthal current, since they are field dependent properties of the HTS tape.

$$R_{sc} = \frac{E_0 l}{I_c}\left(\frac{I}{I_c}\right)^{n-1} \tag{1}$$

A. Current Source

The equivalent circuit model for a current source is displayed in Fig. 4. The V_i block is repeated for all 14 coils. ΣR_{bridge} lumps all series resistances not embedded in voltage tap measurements together. State-space equations are not a function of bridge series resistance. R_{s_i} describes the component of series resistance embedded in voltage tap measurements. This only includes inner coil series resistance and not interface resistance between coils. The system of equations is derived using KVL for each coils closed loop.

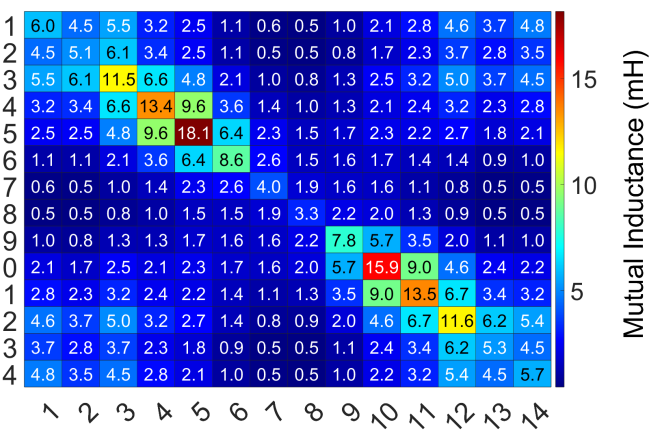

Fig. 3. Mutual Inductance Matrix (mH) heatmap. Coils are ordered 1A-7A, 7B-1B

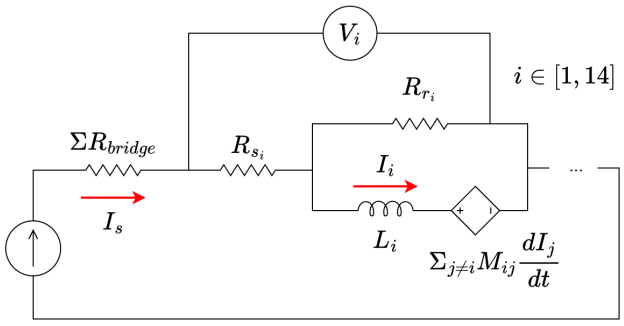

Fig. 4. Current Source circuit model for multiple coupled NI coils.

$$\mathbf{M}\dot{\mathbf{I}} + \operatorname{diag}(\mathbf{R})\,\mathbf{I} = \mathbf{R}I_s(t) \tag{2}$$

$$\dot{\mathbf{I}} = -\mathbf{M}^{-1}\operatorname{diag}(\mathbf{R})\,\mathbf{I} + \mathbf{M}^{-1}\mathbf{R}I_s(t) \tag{3}$$

$$\mathbf{A} = -\mathbf{M}^{-1}\operatorname{diag}(\mathbf{R}) \quad \mathbf{B} = -\mathbf{M}^{-1}\mathbf{R} \tag{4}$$

$$\mathbf{I}(t) = e^{\mathbf{A}t}\mathbf{I}(0) + \int_0^t e^{\mathbf{A}(t-\tau)}\mathbf{B}I_s(\tau)\,d\tau \tag{5}$$

Where $\mathbf{R}$ is the 14x1 column vector of coil radial resistances, $\mathbf{I}$ is the 14x1 column vector of coil azimuthal currents and $I_s(t)$ the series current driven from the power supply.

B. Open Circuit

In the open circuit model (sudden discharge), there is no forced response (Fig. 5). Azimuthal current in each coil discharges radially within each coil.

$$\mathbf{M}\dot{\mathbf{I}} + \operatorname{diag}(\mathbf{R})\,\mathbf{I} = 0 \tag{6}$$

$$\mathbf{I}(t) = e^{\mathbf{A}t}\mathbf{I}(0) \tag{7}$$

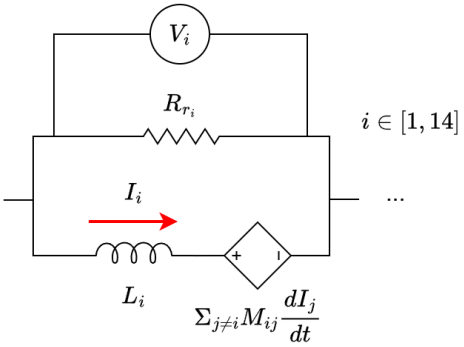

Fig. 5. Open circuit model for multiple coupled NI coils.

IV. Estimation Method

Internal coil series resistances, R_{s_i} were estimated from steady-state voltage measurements, where inductive voltages had decayed to zero, using Ohm's law, $V = IR$. These estimated series resistances were then used as fixed variables in the state-space equations, to estimate radial resistances.

Coil radial resistance was estimated using Non-Linear Least squares, an iterative solver which attempts to minimize the sum of squared residuals. This was implemented by the Python package, SciPy. One can substitute the azimuthal current vector equation to get an equation in terms of coil voltage taps, series current, coil series resistance and the mutual inductance matrix. The remaining unknowns, are the parameters to be estimated. These include:

- $\mathbf{R}$, the 14x1 column vector of coil radial resistances.
- $\mathbf{b}$, the 14x1 column vector of coil voltage tap sensor offsets.

Let $\tilde{\mathbf{y}}$ be the vector of measured coil voltages and β the vector of all estimated parameters ($\mathbf{R}$ and $\mathbf{b}$). Then, $f(\mathbf{I}, \beta)$ can be used to compute the residual (difference between measured and predicted data-points). Note $I_s(t) = 0$ under the Open Circuit model, so these terms are only relevant for the Current Source model.

$$f(\mathbf{I}, \beta) = -\mathbf{R}\mathbf{I} + \mathbf{R}I_s(t) + \mathbf{R}_s I_s(t) + \mathbf{b} \tag{8}$$

We can then substitute eq. 5 or eq. 7 (depending on whether the Current Source or Open Circuit model is used) as $\mathbf{I}$ into eq. 8. Each iteration, the Jacobian matrix, $\mathbf{J}$ is numerically estimated by the solver and is used to steer the solver toward a converged solution.

$$\mathbf{r} = \tilde{\mathbf{y}} - f(\mathbf{I}, \beta) \tag{9}$$

$$\beta^{k+1} = \beta^k + \left(\mathbf{J}^T \mathbf{J}\right)^{-1} \mathbf{r} \tag{10}$$

V. Experimental Method

The experiment was conducted inside a 1.2 m vacuum chamber. The magnet was cooled to 30 K. Coil temperatures remained constant for the duration of the experiment. Although Junior has been designed to be powered by an on-board Superconducting Power Supply (Flux Pump), this experiment was carried out using a conventional TDK-Lambda Power Supply [14], operating as a controlled current source. Experimental voltage data was obtained from three different scenarios, the first two of which, coil radial resistances were estimated. The scenarios are outlined as follows:

- **20 A Step Response** - the TDK-Lambda was stepped from 0-20 A current (essentially instantly).
- **20 A Sudden Discharge** - the TDK-Lambda was stepped from 20-0 A current (essentially instantly).
- **720 A Ramp** - the TDK-Lambda was ramped from 0-720 A current over an 9 hour period. This was not a constant ramp.

VI. Results

Experimental data and curve fits are displayed in Fig. 6-7 and summarized in Table 2. Fits were obtained using the described models and radial resistance estimates obtained from the described estimation method.

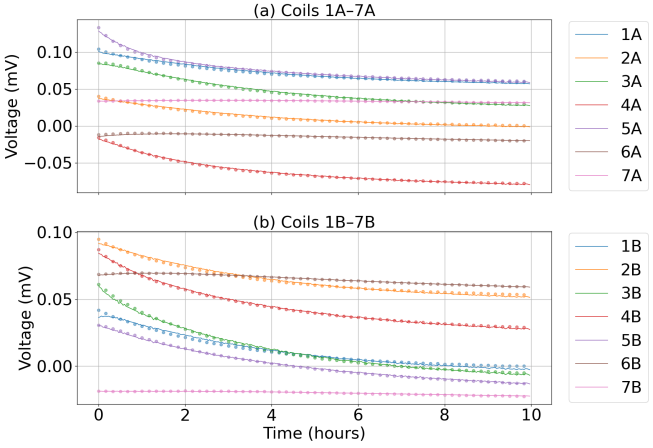

Fig. 6. Fitted and measured coil voltages of Junior coils (a) 1A-7A and (b) 1B-7B for a 20 A step current input.

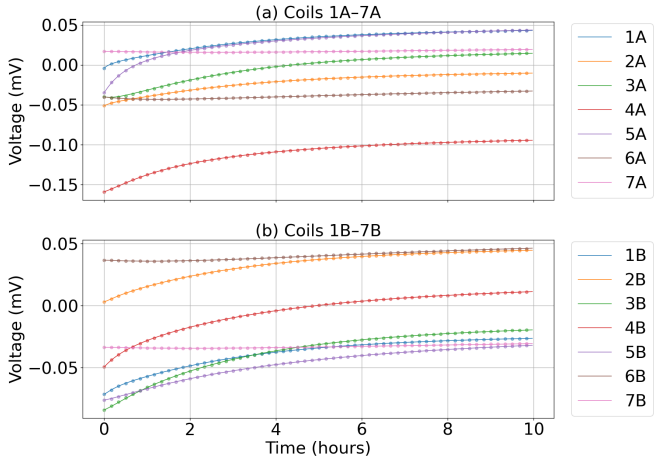

Fig. 7. Fitted and measured coil voltages of Junior coils (a) 1A-7A and (b) 1B-7B for a 20 A sudden discharge

TABLE II
RADIAL RESISTANCE STATISTICS FOR EACH COIL

Coil	20 A Step Fit (μΩ)	20 A Discharge Fit (μΩ)
1A	2.46	7.15
2A	2.14	2.65
3A	3.16	2.97
4A	3.42	3.56
5A	3.93	5.98
6A	0.66	0.68
7A	0.36	0.41
7B	0.39	0.50
6B	0.77	0.57
5B	2.61	2.09
4B	3.21	4.80
3B	3.69	2.45
2B	2.23	1.57
1B	2.16	4.51

The estimated parameters for both the 20 A Step Fit and 20 A Sudden Discharge are used to reconstruct coil voltages of a 720 A current ramp (Fig. 8). Only Coils 1A and 2B are displayed, so it easier to visualize. These were the coils which had a large disagreement between the step and sudden discharge.

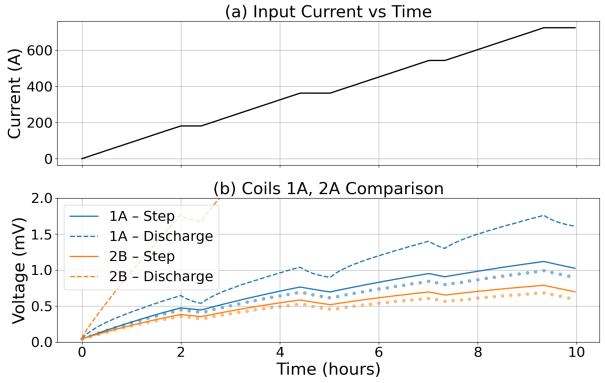

Fig. 8. (a) 720 A current ramp, $I_s(t)$ (b) Fitted and measured coil voltages of Junior coils 1A and 2B constructed using radial resistance estimates from Table 2.

VII. DISCUSSION

Overall, results displayed good agreement between estimated parameters and experimental data. Estimates were consistent across the 20 A step and sudden discharge datasets, for all coils, with the exception of coils 1A and 2B, which are predicted to be unexpectedly large using the sudden discharge model.

Radial resistance estimates obtained from the 20 A sudden discharge resulted in poor reconstruction, specifically coil 1A and 2B, of the 720 A ramp (Fig. 8). This suggests a problem with the sudden discharge model. Alternatively, the 20 A ramp estimates are able to reconstruct the 720 A ramp signals well. However, the reconstruction did grow poorer over time. Several hypotheses are posed to explain this.

- The error seems approximately proportional to time and therefore current, indicating series resistance estimates might be inaccurate.
- The center of the magnet contains an iron shield which may have saturated at higher currents, affecting the mutual inductance matrix. This would render the model invalid at higher currents. In the future, a changing mutual inductance matrix due to saturation of magnetic materials could be included in the fitting process.
- Poor fits could be due to error accumulation within the integral term, as previously suggested. Finally, the current source model includes a cumulative integral which is a function of the inverse of the mutual inductance matrix and radial resistance estimates. Any errors will amplify with time.
- The system is a high dimensional fitting problem with 28 parameters being fit. It is possible that these estimates are overfit. The least squares solver may be stuck in a local minima trap.

Outer coils 6-7 are predicted to have a significant back-current transient, due to their combination of low radial resistance and relatively large inductive coupling with other coils. This result is of interest, as it highlights the affect of radial resistances on the integrated magnet system. Outer coils are designed to ensure a 'zero-field region', required for an on-board Superconducting Power Supply (Flux Pump) to operate. Therefore, the set of coil radial resistances must ensure transient currents keep a 'zero-field region' low enough for which the Flux Pump can operate. The transient response to the 20 A current step input is displayed in Fig. 9.

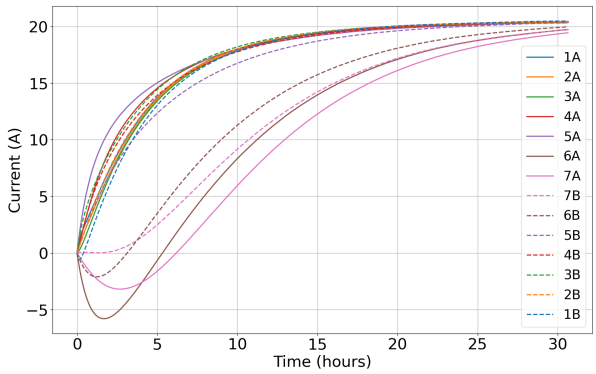

Fig. 9. Predicted azimuthal current transient from predicted radial resistances in response to 20A step. Note the back-current in outer coils 6 and 7.

This paper only considers a single gradient descent based estimation method. Future work including different coil arrangements and estimation methods would be valuable.

VIII. CONCLUSION

A method was proposed for estimating the radial resistance of inductively coupled NI HTS coils and was used to estimate the radial resistances for each of Junior's 14 coils. Overall, the results showed good agreement between the estimated parameters and experimental data. Estimates were consistent across all considered datasets for all coils, with the exception of coils 1A and 2B. While these results are of specific interest for dipole fusion magnets, the estimation approach can be applied to any magnet comprised of multiple NI HTS coils. Further efforts to validate the proposed approach are necessary.

REFERENCES

[1] A. Hasegawa, Liu Chen, and M.E. Mauel. "A D-3He fusion reactor based on a dipole magnetic field". In: *Nuclear Fusion* 30.11 (Nov. 1990), p. 2405. DOI: 10.1088/0029-5515/30/11/018.

[2] A. Hasegawa. "A dipole field fusion reactor". In: *Comments on Plasma Physics and Controlled Fusion* 11 (11 Nov. 1987), pp. 147–151. ISSN: 0374-2806.

[3] AC. Boxer et al. "Turbulent inward pinch of plasma confined by a levitated dipole magnet". In: *Nature Phys* (6 Jan. 2010), pp. 207–212. DOI: 10.1038/NPHYS1510.

[4] J. Morikawa et al. "Development of a super-conducting levitated coil system in the RT-1 magnetospheric confinement device". In: *Fusion Engineering and Design* 82.5 (2007). Proceedings of the 24th Symposium on Fusion Technology, pp. 1437–1442. ISSN: 0920-3796. DOI: https://doi.org/10.1016/j.fusengdes.2007.03.050.

[5] S. Hahn et al. "HTS Pancake Coils Without Turn-to-Turn Insulation". In: *IEEE Transactions on Applied Superconductivity* 21.3 (2011), pp. 1592–1595. DOI: 10.1109/TASC.2010.2093492.

[6] Yuqian Li et al. "Feasibility Study of the Impregnation of a No-Insulation HTS Coil Using Solder". In: *IEEE Transactions on Applied Superconductivity* 28.1 (2018), pp. 1–5. DOI: 10.1109/TASC.2017.2773831.

[7] E.-K. C. Brewerton et al. "From Modelling to Application: Exploring Quench Tolerance in High-Field HTS Magnets". In: *IEEE Transactions on Applied Superconductivity* (2025). DOI: 10.1109/TASC.2025.3635639.

[8] Craig S. Chisholm et al. *Design and initial results from the "Junior" Levitated Dipole Experiment*. 2025. arXiv: 2508.17691 [physics.plasm-ph]. URL: https://arxiv.org/abs/2508.17691.

[9] S. Venuturumilli et al. "Modeling HTS non-insulated coils: A comparison between finite-element and distributed network models". In: *AIP Advances* (13 Mar. 2023). DOI: 10.1063/5.0135291.

[10] X. Wang et al. "Turn-to-Turn Contact Characteristics for an Equivalent Circuit Model of No-Insulation ReBCO Pancake Coil". In: *Superconductor Science and Technology* 26.3 (2013), p. 035012. DOI: 10.1088/0953-2048/26/3/035012.

[11] Konstantinos Bouloukakis et al. "Discharge Behaviour and Modelling of a 1.5 T REBCO Magnet with Quench Tolerant Coils Impregnated with Conductive Epoxy". In: *IEEE Transactions on Applied Superconductivity* 31.5 (2021). Cited by: 12; All Open Access, Green Open Access. DOI: 10.1109/TASC.2021.3059975.

[12] J.R. Olatunji et al. "Modelling the Quench Behavior of an NI HTS Applied-Field Module for a Magnetoplasmadynamic Thruster Undergoing a 1kW Discharge". In: *IEEE Transactions on Applied Superconductivity* 33.5 (2023). Cited by: 7. DOI: 10.1109/TASC.2023.3264170.

[13] COMSOL Multiphysics. "Introduction to COMSOL multiphysics®". In: *COMSOL Multiphysics, Burlington, MA, accessed Feb* 9 (1998), p. 2018.

[14] TDK-Lambda Corporation. *GSP10-1500 Programmable DC Power Supply Datasheet*. Accessed: 2025-10-13. TDK-Lambda Corporation. Shibaura Renasite Tower, 3-9-1 Shibaura, Minato-ku, Tokyo 108-0023, Japan, 2022. URL: https://product.tdk.com/en/search/power/switching-power/prg-power/info?part_no=GSP10-1500-3P400.